university of groningen

faculty of science and engineering

Trapping Nanoparticles: Simulations of a Dual-Frequency Paul Trap

Author:
Alberto GUSI
(s5066174)

Supervisor:
prof.dr. Steven HOEKSTRA
Second examiner :
dr. Jelle BLIJLEVEN

Bachelor's Thesis
To fulfill the requirements for the degree of
Bachelor of Science in Physics
at the University of Groningen

June 29, 2025

Abstract

Paul traps are devices widely used in physics, from mass spectrometry to quantum computing and nanoparticle manipulation. This study investigates the optimal operational parameters, namely the voltage amplitude and frequency of the power sources, for a dual-frequency Paul trap to stably confine a charged nanoparticle. Using *COMSOL Multiphysics*, the electric field produced by the trap's electrodes and the particle dynamics are simulated under varying voltage and frequency conditions. The simulations' outcomes are compared to theoretical calculations to prove their reliability. Stable confinement in the radial plane is achieved using two power sources: one of 100 V at 20 MHz and the other in the range of 1000–1600 V at 3 kHz. Axial confinement is achieved using two endcaps electrodes, which give successful results limited to a single voltage configuration. The simulations also estimated the trap's potential depth, reaching over 500 eV. These results support the trap's use as a backup mechanism for optical tweezers and a basis for future multi-species trapping experiments.

Contents

1 Introduction

Since the early 1950s, many physicists have devoted their careers to studying and developing various techniques aimed at isolating single molecules, ions, and nanoparticles from the surrounding environment. Two pivotal inventions that have significantly advanced this field, facilitating remarkable discoveries, are optical tweezers and the Paul trap.
Optical tweezers, first invented by Arthur Ashkin in the 1970s, operate by tightly focusing a laser beam to create a high-intensity optical gradient force. When a dielectric particle is placed in the laser focus, it experiences a force that pulls it toward the region of highest light intensity. This occurs due to the interaction between the induced electric dipole in the particle and the spatial variation in the light's electric field [1]. Thanks to this invention, Ashkin was awarded the 2018 Nobel Prize in Physics.
Conversely, a Paul trap utilizes an electric field generated by alternating and direct current voltages to establish a quadrupole potential, confining charged particles within the trapping region [2]. This technology, invented by Wolfgang Paul in 1954, earned him the Nobel Prize in Physics in 1989.

Nowadays, the control and manipulation of micro and nano objects are of considerable importance across various sectors. In medicine, this technology is used for the study of individual proteins [3], bacteria [4] and viruses [5]. In physics, the aforementioned traps are utilized for mass spectroscopy [6], quantum information processing [7], and potentially as pivotal tools for the detection of millicharged dark matter. These tools have been employed to levitate nanoparticles of hundreds of nanometers in diameter and cool them sufficiently to be controlled at the quantum level, thereby enabling the study of macroscopic quantum physics [8].

Although both techniques ultimately have the same purpose, they have been applied differently over the years and have been refined to enhance accuracy and stability, adapting to various contexts. Due to its underlying physical principles, a Paul trap offers deeper potential energy (1 keV) and a larger trapping volume (1 cm^3) [9] compared to optical tweezers (1 eV, 1 μm^3) [10], making it more suitable for certain applications, such as the simultaneous trapping of multiple particles or interactions among different species [11] [12]. Recently, hybrid systems incorporating both traps have been developed to leverage the advantages of each [13]. In these systems, optical tweezers serve as the primary trapping mechanism, while the Paul trap functions as a safety net to retain the particle and reposition it at the laser focal point if it escapes from the tweezers.

In this study, the functioning of a Paul trap is investigated. The trap is combined with an optical tweezer and analyzed through numerical simulations. Particularly, its aim is to work as a safety measure for the optical tweezer. In fact, as aforementioned, the Paul trap offers a significantly deeper potential well and a much larger trapping volume than an optical tweezer. When combined with the latter, the Paul trap can effectively retrap nanoparticles that escape from the optical potential, thereby ensuring system stability and enabling longer experimental runtimes. Furthermore, by driving the trap electrodes with different RF sources, the Paul trap can be configured to simultaneously confine different types of nanoparticles, enabling multi-species trapping for future experiments.
The trap's geometry is adapted to align with the configuration of the optical tweezer, which serve as the primary trapping instrument. Simulations of the electric field generated by the trap's electrodes are conducted using the software *COMSOL Multiphysics* , which also allows to simulate the particle trajectory within the field.

1.1 Research Question

This study seeks to determine the optimal operational parameters for a Paul trap that can be used combined with an optical tweezer or alone for simultaneous trapping of two particles. Given these goals, the research question for this study is: *Using a daul-frequency RF Paul trap, what voltages and frequencies should be applied to the electrodes to achieve stable confinement of a charged nanoparticle?*

2 Theoretical Background

2.1 Principle of Paul Trap

To trap a particle in free space a dynamic electric potential has to be created. In fact, according to Earnshaw's theorem, *'Charged particles cannot be held in stable equilibrium by electrostatic forces alone'* [14]. Furthermore, according to electrodynamics, any potential in free space has to satisfy the Laplace's equation $\nabla^2\Phi = 0$ [14]. To satisfy these conditions, the potential created by a Paul trap has the form:

$$\Phi = \frac{\Phi_0}{2r_0^2}(\alpha x^2 + \beta y^2 + \gamma z^2), \tag{1}$$

where Φ_0 is the potential applied to the electrodes and r_0 is the characteristic half-diagonal distance between the electrodes of the Paul trap. Then, $\alpha + \beta + \gamma = 0$ is the necessary condition to satisfy $\nabla^2\Phi = 0$.
Among the various permissible combinations of coefficients that satisfy the governing conditions, certain conventional choices are often adopted for practical applications. A commonly employed set includes $\alpha = -\beta = 1$ and $\gamma = 0$, which yields a potential of the form $\Phi = \frac{\Phi_0}{2r_0^2}(x^2 - y^2)$. This configuration satisfies Laplace's equation and is characteristic of the electric quadrupole field utilized in Paul traps. As can be noted, this is a 2D potential and is effectively used to achieve in-plane confinement (in this case in the xy-plane). Out-of-plane confinement is achieved by applying DC voltages to two endacap electrodes which are placed along the z-direction. The trap's geometry can be seen in Figure 7.
In Equation (1), the applied potential is given by:

$$\Phi_0 = U + V\cos(2\pi f \cdot t), \tag{2}$$

where U is a static DC voltage and V is the voltage amplitude oscillating with frequency f. The electric field generated in the xy-plane is calculated from $E = -\frac{d\Phi}{dx}$ and $E = -\frac{d\Phi}{dy}$. By multiplying the field by the charge, the force acting on the particle can be found. Given the particle's mass m and charge Q, its equations of motion in the trap are given by:

$$\ddot{x} + \frac{Q}{mr_0^2}(U + V\cos(2\pi f \cdot t))x = 0, \tag{3}$$

$$\ddot{y} - \frac{Q}{mr_0^2}(U + V\cos(2\pi f \cdot t))y = 0. \tag{4}$$

Since cosine is an even function, Equations (3), (4) can be generalized as:

$$\ddot{\psi} + (a + 2q\cos(2\pi f \cdot t))\psi = 0, \tag{5}$$

where ψ represents a generalized spatial coordinate (i.e. x-, y- or z-direction). Equation (5) has the form of a Mathieu equation where:

$$a = \frac{4QU}{mr_0^2(2\pi f)^2} \qquad q = \frac{2QV}{mr_0^2(2\pi f)^2}, \tag{6}$$

are the so called stability parameters. In addition, when substituting ψ with the x- and y-direction, the following relations are obtained:

$$q_x = -q_y \qquad a_x = -a_y. \tag{7}$$

Proving the derivation and solving the Mathieu equation is a tedious process that goes beyond the scope of this research. An exhaustive and detailed explanation can be found in [15]. Of primary importance in the context of particle dynamics within a Paul trap are the stability parameters a and q. These parameters determine the nature of the solutions to Equations (3) and (4), with the motion either exhibiting infinite growth or remaining confined within the trap, depending on their values. The stability regions corresponding to bounded solutions can be effectively visualized by plotting a graph of a versus q, where each stable pair is represented, as illustrated in Figure 1.

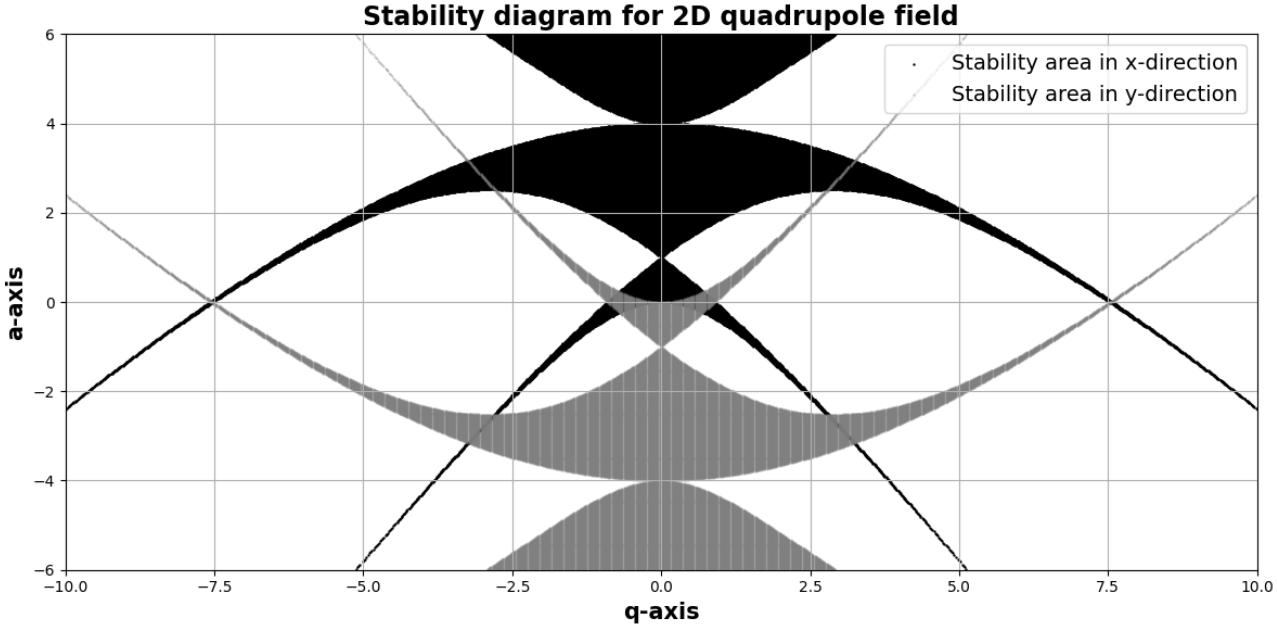

Figure 1: Stability diagram of the Mathieu equation. The solutions are stable in the black and grey areas for the x- and y-direction respectively.

Furthermore, by exploiting the symmetries outlined in Equation (7), it becomes evident that the stability region in the y-direction is the mirror image of the x-direction stability region across the origin. Consequently, stable confinement of a particle in the xy-plane requires that the parameters a and q lie within the intersection of the respective stable regions for both axes. For Paul traps, the usual operating regime is for values close to the origin [12]. This intersection, representing the domain of simultaneous stability, is depicted in Figure 2.
Consequently, to trap a particle with a given charge to mass ratio in the xy-plane of a Paul trap with a specific characteristic distance r_0, the applied voltages and their frequencies have to be chosen such that the calculated stability parameters fall in the area highlighted in Figure 2.

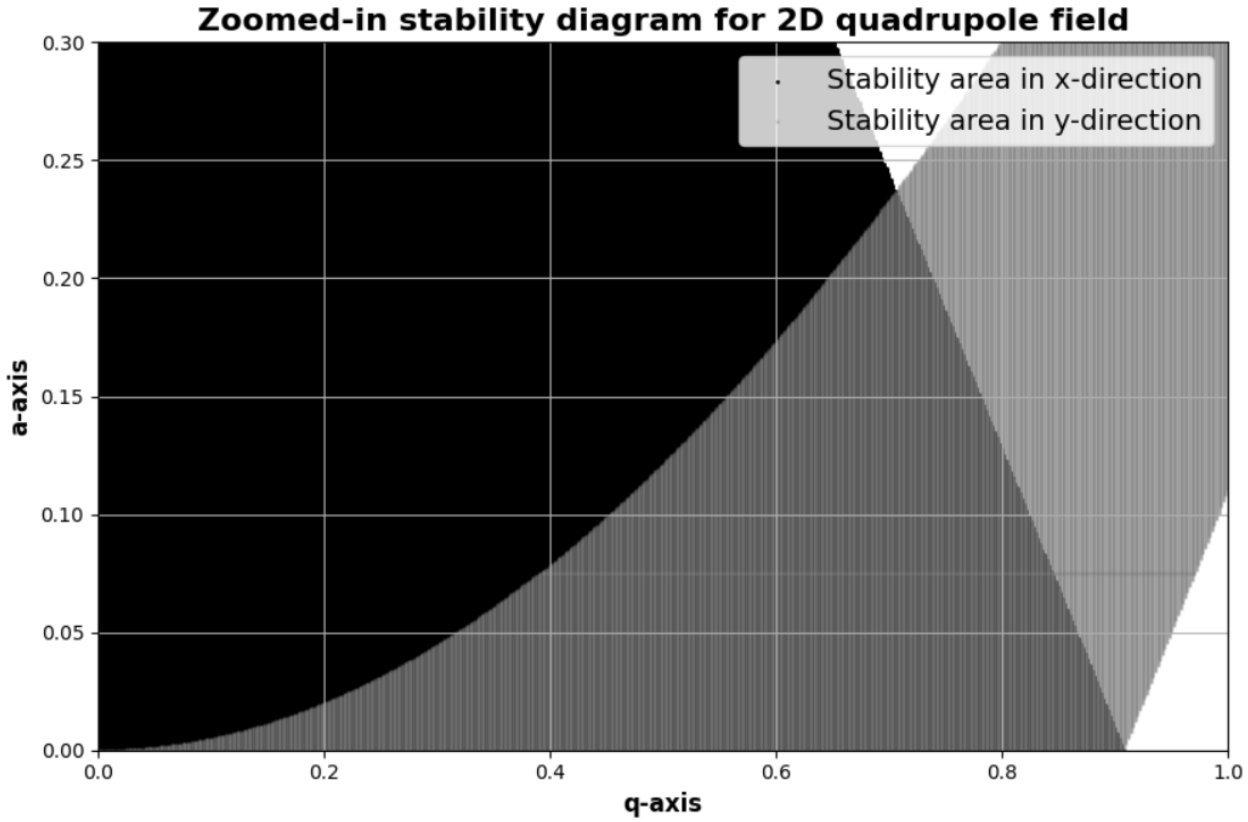

Figure 2: The region where the stable areas in both the x- and y-directions overlap represents the set of solutions that are simultaneously stable in both directions. The highest q-value at which the two graphs overlap is $q = 0.900$.

2.2 Conditions for Simultaneous Trapping of an Ion and a Nanoparticle

Conventional Paul traps are typically optimized to confine particles with a specific charge-to-mass ratio. In such configurations, the DC and RF voltages are selected to ensure that only particles with predetermined properties can be levitated within the trap when it is operational. While this setup is relatively straightforward to implement, it inherently restricts the range of particle species that can be effectively trapped.

To address this limitation, alternative configurations have been developed. In particular, a dual-frequency Paul trap, powered by two independent RF voltage sources, has demonstrated the capability to simultaneously confine a silica nanoparticle and a calcium ion with charge-to-mass ratios of six orders of magnitude difference [11].

This is achieved by driving the two RF sources at significantly different frequencies: one operating in the kilohertz (kHz) range and the other in the megahertz (MHz) range. The resulting potential in the xy-plane produced by such a system is described by:

$$\Phi(x,y) = (V_{slow}\cos(2\pi f_{slow}t) + V_{fast}\cos(2\pi f_{fast}t))\frac{x^2-y^2}{2r_0^2}, \tag{8}$$

where f_{slow} and f_{fast} are the frequencies of the sources (in units of Hertz) and V_{slow} and V_{fast} their amplitudes. A visual representation of this potential can be seen in Figure 3.

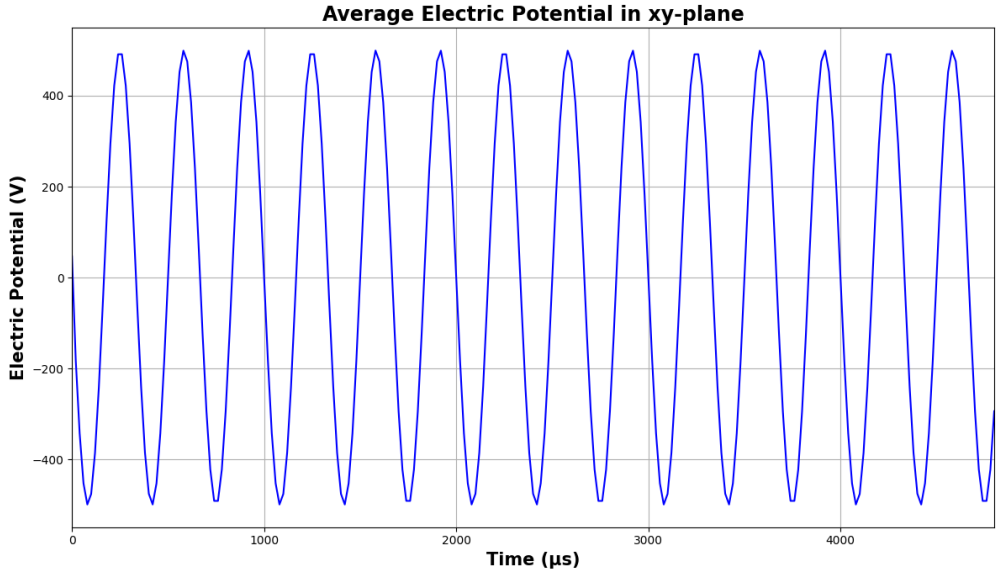

Figure 3: Average electric potential generated by the electrodes in the xy-plane. The applied voltages are V_{slow}=1000 V and V_{fast}=100 V with frequencies of 3 kHz and 20 MHz respectively.

When analyzing the motion of a nanoparticle within this trap, the electric field acting on the particle in a given direction can be determined by computing the spatial derivative of the potential along that direction. Once the directional component of the force is established, the corresponding equation of motion can be derived. Along the x-axis, the resulting equation of motion is given by:

$$m_n\ddot{x} = -Q_n(V_{slow}\cos(2\pi f_{slow}t) + V_{fast}\cos(2\pi f_{fast}t))\frac{x}{r_0^2}, \tag{9}$$

where m_n and Q_n are the mass and charge of the trapped nanoparticle. By neglecting the fast oscillating field, the nanoparticle's oscillation frequency in the trap due to the slow voltage is given by:

$$\omega_n|_{f_{slow}} = \frac{2Q_nV_{slow}}{2\sqrt{2}m_nr_0^2 \cdot 2\pi f_{slow}}. \tag{10}$$

Conversely, by neglecting the slow field, the oscillating frequency calculated in terms of $\omega_n|_{f_{slow}}$ is found to be:

$$\omega_n|_{f_{fast}} = \frac{2\pi f_{slow}V_{fast}}{2\pi f_{fast}V_{slow}}\omega_n|_{f_{slow}}. \tag{11}$$

When substituting the appropriate values of the driving voltages and their frequencies in Equation (11), it can be observed that the fast voltage acts only as a perturbation on the motion of a nanoparticle.

On the other hand, when considering the motion of the ion in the potential field, if the condition $f_{slow} \ll f_{fast}$ is satisfied, the ion sees the slow field as a slowly varying DC force. Its equation of motion can be mapped into a Mathieu equation of the form:

$$\ddot{x} + (a + 2q\cos(2\pi f_{fast} \cdot t))x = 0. \tag{12}$$

The stability parameters in Equation (12) are respectively:

$$a = \frac{4Q_i V_{slow}}{m_i r_0^2 (2\pi f_{fast})^2} \qquad q = \frac{2Q_i V_{fast}}{m_i r_0^2 (2\pi f_{fast})^2}, \tag{13}$$

where m_i is the mass of the ion and Q_i its charge. Given the stability parameters in Equation (13), simultaneous trapping of a nanoparticle and an ion is achieved when [11]:

$$q \ll 1 \qquad |a| < \frac{q^2}{2}. \tag{14}$$

2.3 Parametric Feedback Cooling

Once the particle is trapped, the center of mass motion motion has to be cooled enough to reduce its oscillations to amplitudes of fractions of the diameter. In addition, if the trap is being used as a safety net for the optical tweezers, the particle has to be placed back at the center of the Paul trap, which corresponds to the focal point. To do so, parametric feedback cooling is utilized.
The principle of this cooling technique is to modulate the trap stiffness, depending on the particle position and direction of movement. Particularly, the trap stiffness is increased when the particle is heading away from the trap center, so that the potential wells the particle has to climb are steeper and consequently the particle slows down and eventually moves back. Conversely, when the particle is moving towards the trap center, the stiffness is decreased. This technique has also been used in optical tweezer to cool the center of mass motion of a trapped nanoparticle in ultrahigh vacuum condition [10]. A visualization of this process can be seen in Figure 4.

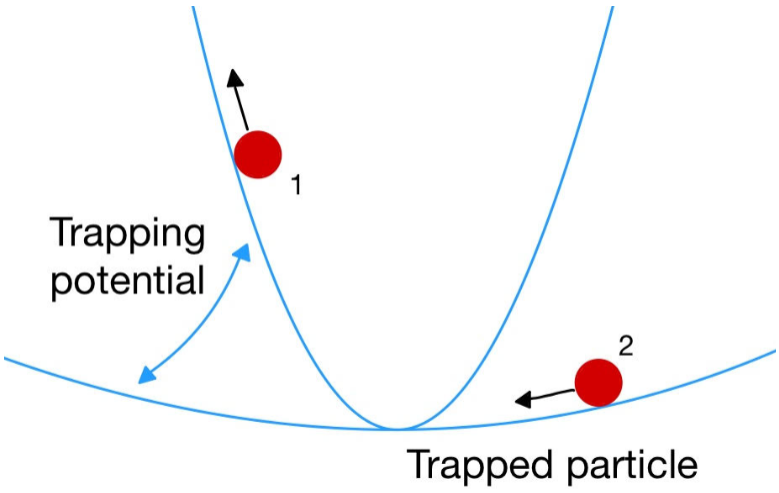

Figure 4: Time varying potential of the trap. The potential walls are increased then the particle is moving away from the center (position 1) and are decreased when the particle is moving towards the center (position 2).

3 Trap Configuration & Simulation Details

3.1 Integration of the Paul Trap within the Optical Trapping System

As mentioned in the introduction, the Paul trap examined in this study is part of a larger experimental framework involving the optical trapping of nanospheres with optical tweezers. The optical trapping setup consists of several essential components: a trapping laser, a vacuum chamber, a microscope objective, and a detection system. For the interested reader, a more detailed explanation of the optical tweezers experimental setup can be found in [1]. In this configuration, the Paul trap must be precisely aligned with the focal point of the laser beam, which is the location at which the nanoparticle is optically confined.
Therefore, it is placed into the vacuum chamber, positioned between the microscope objective and the aspheric collection lens. Figure 5 illustrates the components inside the vacuum chamber.
The four trap electrodes are fixed in place by a holder made of PEEK (Polyether Ether Ketone).
Regarding the physical geometry of the Paul trap itself, it consists of four cylindrical electrodes, each measuring 0.875 mm in radius, with rounded tips. The electrodes are symmetrically arranged about the origin, with a separation of 3.6 mm between the tips of opposing electrodes. This distance corresponds to $2r_0$, as defined in Equation (1). Each electrode is inclined at an angle of 29° with respect to the x-axis. The trap utilized can be seen in Figure 6. Throughout this work, the xy-plane will be considered the radial plane, where the electrodes are located, while the z-direction will be treated as the axial direction, orthogonal to the electrode plane.

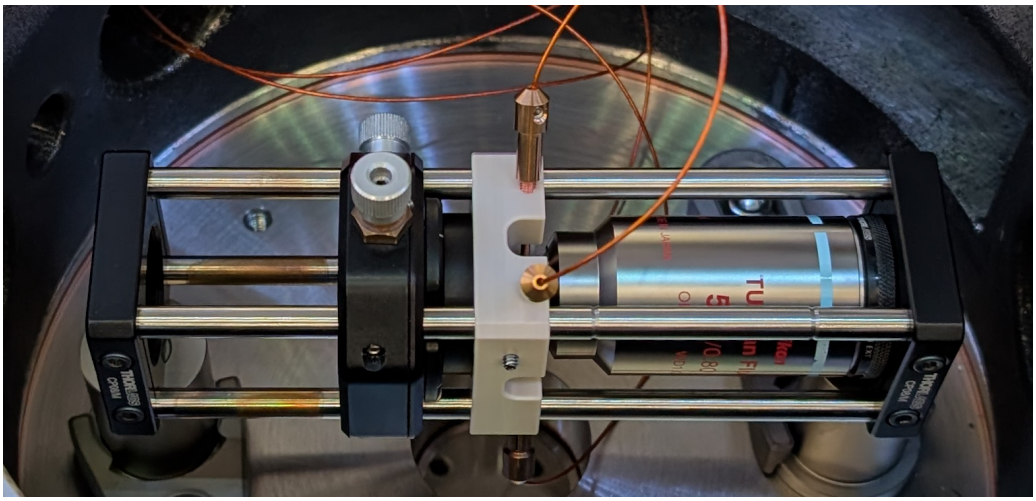

Figure 5: Visualization of the components inside the vacuum chamber. From right to left: the microscope objective, the electrode holder with four electrodes and the collection lens.

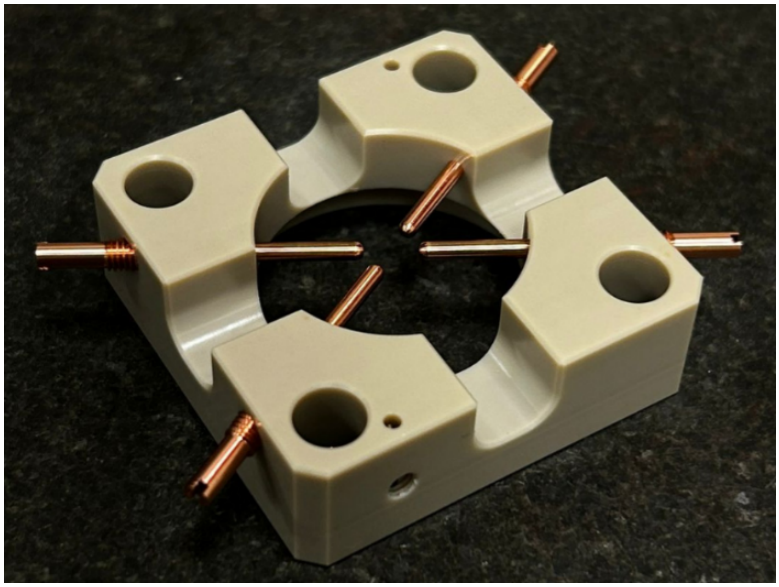

Figure 6: Visualization of the electrodes that compose the Paul trap and respective mount.

3.2 Operation of the Paul Trap and Particle Properties

This study simulates a Paul trap powered by two distinct RF sources. Although the trap is currently used to trap a single nanoparticle at a time, the use of two separate oscillating voltages lays the foundation for future applications involving the simultaneous trapping of two different particle species as outlined in the theory section above.
One pair of opposing electrodes, hereafter denoted as *fast voltage*, is supplied with a voltage oscillating at a frequency of 20 MHz, while the other pair has a driving voltage oscillating at a frequency of 3 kHz, which will be called *slow voltage* from now on. In order to analyze various aspects of the Paul trap's behavior and performance, the amplitude of the voltages supplied to these electrodes will be varied. This adjustment of both the fast and slow voltages will allow to investigate their effects on particle confinement, stability, and the overall trapping characteristics. Moreover, two additional hollow ring electrodes are added in the simulations. These electrodes, named *endcap electrodes*, are used to confine the particle along the z-direction and are powered by a DC voltage of 50 V, as similar to another work [13].

The simulated nanoparticle has a mass of 2.77 fg and a total charge of $5e$. These values are based on the actual mass and charge of typical silica (SiO_2) nanoparticles which are captured in the optical tweezers experiment [1]. This ensures the simulation realistically represents the properties of a particle that could be trapped with the Paul trap.

3.3 COMSOL Configuration for Simulations

To investigate the behavior of the trap and analyze the trajectory of a nanoparticle under different voltages and frequencies applied, computational simulations are performed using the software *COMSOL Multiphysics (version 6.2)*. This software enables the modeling of the electric field generated by the electrodes when subject to specific voltages, which can be set by the user. Additionally, it allows for the simulation of a charged particle's motion within the computed electric field, which can be

dynamically visualized through real-time animation.

The simulation is conducted using two physics interfaces: **Electrostatic** to simulate the electric field produced by the electrodes and **Charged Particle Tracing** to simulate the dynamics of the nanoparticle subjected to this electric field. Prior to running the simulation, the geometry of the Paul trap must be constructed. This is accomplished directly in *COMSOL* using the geometry section in the toolbar. In this study, the trap built has the following parameters:

Name	**Value**	**Description**
Theta	29°	Angle between electrodes
R_electrode	$8.75{\cdot}10^{-4}$ m	Radius of electrodes' tip
R_inner	0.0036 m	Ring electrodes' inner radius
R_outer	0.0053 m	Ring electrodes' outer radius
H_ring	0.00044 m	Ring electrodes' height

Table 1: List of parameters used in *COMSOL* to build the trap's geometry. The parameters are used to automate the building process. If a value is changed, then all the geometry will change accordingly.

To simplify the building process, the 2D cross section of the top left electrode is drawn in the xy-plane using the **Work Plane** tool in *COMSOL*. This 2D profile is then revolved 180° about its axis to generate the full 3D electrode structure.
Given the symmetry of the trap with respect to both the x-axis and the y-axis, it is sufficient to model one electrode. The remaining three electrodes are then generated by applying mirror operations across the x-axes and y-axes. The endcaps electrodes are built using as an inner radius, outer radius and height the parameters R_inner, R_outer and H_ring given in Table 1 respectively. These values are chosen to ensure that the endcaps provide optical access for the optical tweezer's laser beam.
Moreover, the vacuum chamber in which the trap is placed must also be modeled, as it represents the environment where the nanoparticle will move. To do so, a cylinder with a radius of 15 mm and a height of 25 mm encapsulating the entire Paul trap is created. The final geometry as created in *COMSOL* is visualized in Figure 7.
Next, materials are assigned to each component. All electrodes are made of copper, while the vacuum chamber is assigned the *'Perfect Vacuum'* material available in the material library.

The 'Electrostatics' module is configured to simulate the desired electric field. Three **Terminal** boundary conditions are applied: two are assigned to the opposing pairs of electrodes, and the third to the endcap electrodes. The opposing electrodes are supplied with time-varying voltages of the form $V = V_{fast} \cdot \sin(2\pi f_{fast} t)$ and $V = -V_{slow} \cdot \sin(2\pi f_{slow} t)$ for the fast voltage and slow voltage respectively. The endcaps electrodes are supplied with a static DC voltage of 50 V.
To track the motion of the nanoparticle within the vacuum chamber, the 'Charged Particle Tracing' module is used. To couple the particle's motion to the electric field, the boundary condition **Electric Force** is selected. In its settings, the Electrostatics module is specified as the origin of the force. This ensures that *COMSOL* applies the previously defined electric field as the acting force on the nanoparticle within the vacuum chamber. Furthermore, a **Release from Grid** feature is added to define the initial position and velocity of the nanoparticle at the start of the simulation. In all the simulations performed, the particle's initial position corresponds with the trap's center, hence the $(0\hat{x},0\hat{y},0\hat{z})$ coordinates. A **Particle Properties** node is also included to assign the particle's mass and charge.

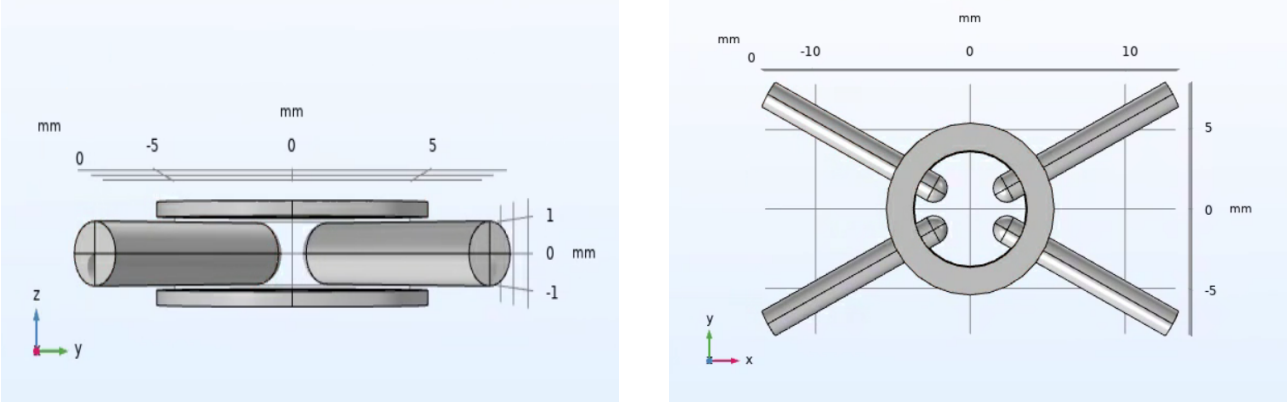

(a) (b)

Figure 7: Trap geometry visualized in *COMSOL*. (a) Side view of the trap. (b) Top view of the trap. The cylindrical enclosure has been omitted to enhance the visibility of the electrodes. The coordinate system is shown in the bottom-left corner of each view.

Finally, two studies are set. The first is used to run the simulation of the electric field, while the second one is used to track the particle motion in the vacuum chamber. Throughout this study, a time range going from 0 μs to 1000 μs in steps of 20 μs is used for the simulations as it is observed to be the best trade of between computational time and resolution of the results.

4 Results

4.1 Analysis of Particle Stability in the xy-Plane

The first thing done in the analysis of the Paul trap is to verify that the condition stated in Equation (11) holds true. Therefore, the values for which the trap is operated are substituted in the equation. The following result is derived:

$$\omega_n|_{f_{fast}} = \frac{3000 \cdot 100}{20 \cdot 10^6 \cdot 1000}\omega_n|_{f_{slow}} = 2.5 \cdot 10^{-6}\omega_n|_{f_{slow}}. \tag{15}$$

This shows that the fast frequency is only a fraction of the slow frequency. Consequently, when only a nanoparticle is trapped, the fast voltage can be considered as a DC force and its amplitude can be plugged in the stability parameters given by Equation (6) as U.

To determine if the particle remains confined in the xy-plane, the stability parameters defined in Equation (6) are calculated for various values of V_{slow}, keeping the driving frequencies and V_{fast} constant. The results are summarized in Table 2. Each pair of values is then plotted in the stability graph visible in Figure 8 to check whether they lie in the stability zone.

To verify the theoretical prediction, 2D simulations are run over a time interval of 4800 μs. The particle's motion is visualized through animations. Additionally, graphs of the x- and y-position against time are plotted to show when the particle escapes the trapping region. Two of these graphs, which correspond to the limit cases, are presented in Figure 11 and Figure 12 given in the Appendix.

$\mathbf{V}_{slow}$**(V)**	$\mathbf{V}_{fast}$**(V)**	**a**	**q**	**Particle Trapped**
1000	100	0.100	0.502	Yes
1100	100	0.100	0.553	Yes
1200	100	0.100	0.603	Yes
1300	100	0.100	0.653	Yes
1400	100	0.100	0.703	Yes
1500	100	0.100	0.753	Yes
1600	100	0.100	0.803	Yes
1700	100	0.100	0.854	No
1800	100	0.100	0.904	No
1900	100	0.100	0.955	No

Table 2: Theoretically calculated stability parameters corresponding to various applied slow voltages. The slow and fast driving frequencies are fixed at 3 kHz and 20 MHz, respectively. The last column states whether the particle was observed to be trapped or not in the simulations.

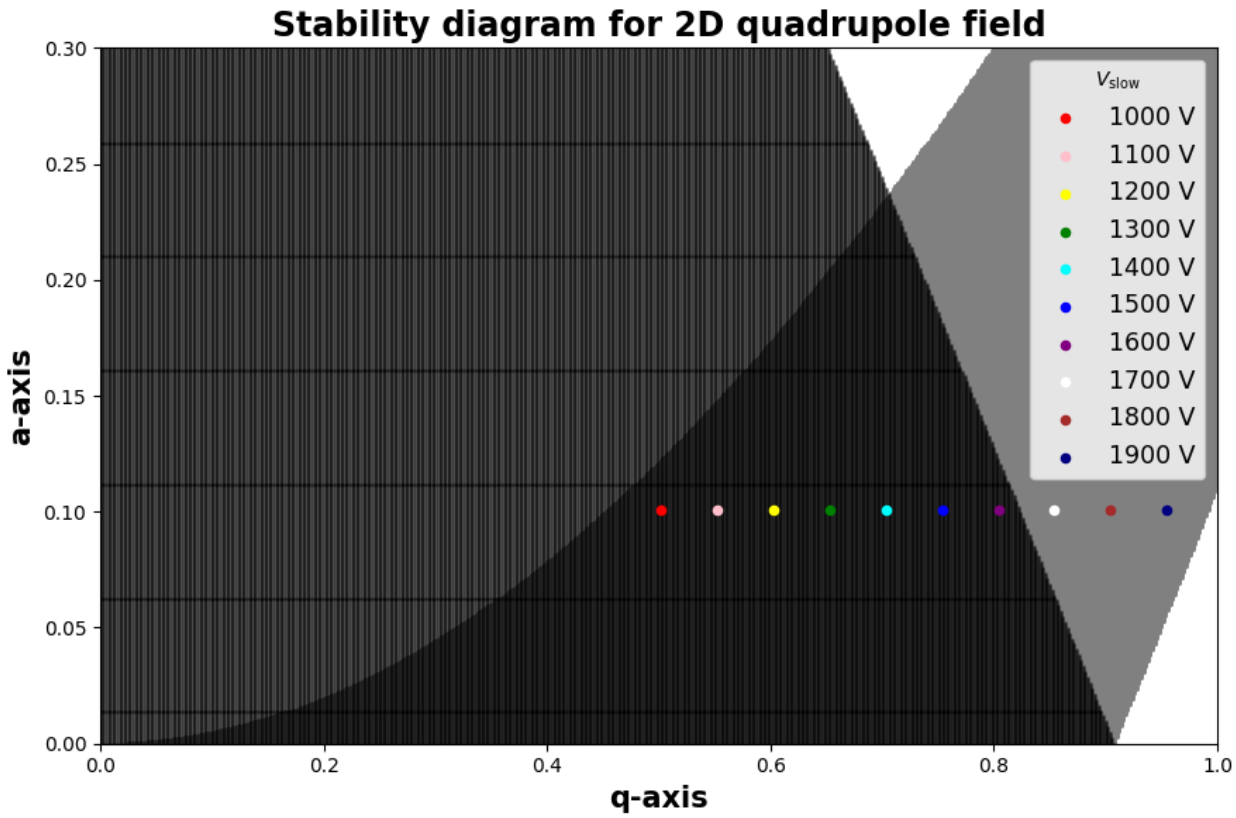

Figure 8: The colored points represent the calculated a and q values for different values of *slow voltage* while the *fast voltage* is kept the same.

4.2 Axial Confinement and Estimation of Trap Depth

To check stable confinement along the z-direction, 3D simulations are run. Due to a longer computational time, these simulations span a time range of 700 μs, such that two periods of the *slow voltage* are included. To analyze the particle's motion, animations are observed and graphs of the z-position over time are plotted. As an example, Figure 9 shows the obtained plot for applied V_{slow}=1100 V and V_{fast}=100 V.

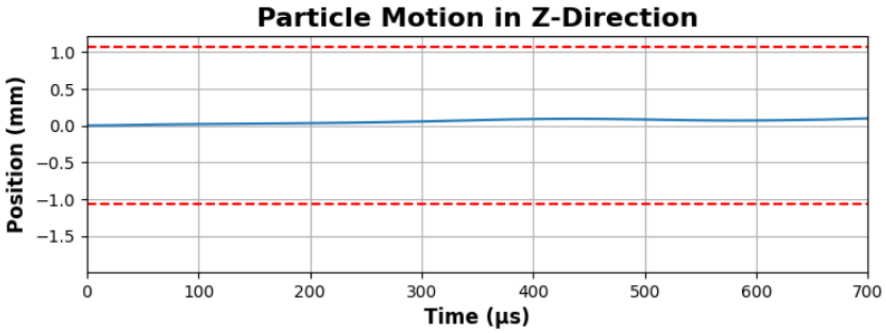

Figure 9: Graph of the z-position of the particle as a function of time. The two horizontal dashed lines represent the z-limit of the trapping region.

From Figure 9 it is observed that the particle remains trapped throughout the whole simulation, with small displacement from the center along the z-direction. However, the particle does not remain

trapped in the z-direction for all applied voltages. The graphs for the rest of the voltages are reported in Figure 13 given in the Appendix.

Furthermore, the trapped particle's kinetic energy is analyzed to estimate the potential trap's depth. For each applied voltage that results in stable confinement, the maximum particle's kinetic energy calculated by *COMSOL* are reported in Table 3. For these measurements, V_{fast} is also varied to investigate its influence on the trap depth. These values are plotted in a graph of the energy against the slow voltage, visible in Figure 10, to determine the voltage combinations that yield the deepest trapping potential.

$\mathbf{V}_{slow}$**(V)**	**Kinetic Energy (eV) for** $V_{fast} = 85$**V**	**Kinetic Energy (eV) for** $V_{fast} = 100$**V**	**Kinetic Energy (eV) for** $V_{fast} = 115$**V**
1000	237.5	277.5	154.6
1100	359.1	256.0	166.5
1200	419.4	406.2	229.5
1300	310.9	371.8	145.6
1400	494.4	274.2	252.0
1500	384.3	375.3	209.8
1600	437.5	552.1	390.2

Table 3: Maximum kinetic energies computed in the simulations.

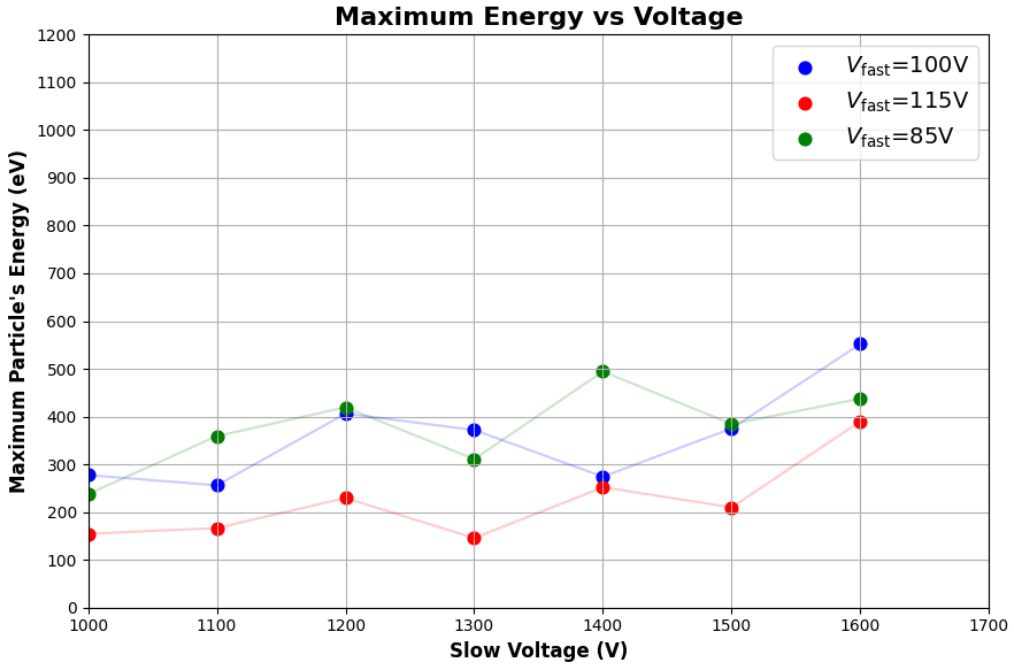

Figure 10: Values of the maximum particle's kinetic energy for different values of V_{slow} and V_{fast}. The frequencies are still fixed at 3 kHz and 20 MHz respectively.

5 Discussion

The aim of this project was to investigate the functioning of a Paul trap, such that it can be used to retrap a nanoparticle in the eventuality it escapes from the trapping potential of the optical tweezer. The entire analysis was conducted computationally, using simulation tools to determine optimal operational parameters without the need for physical experimentation.

Through theoretical formula and finite element simulations, the required voltages to confine a nanoparticle in the xy-plane of the trap were determined, given fixed frequencies of 3 kHz and 20 MHz.These voltage values are consistent with those reported in similar study [11], although they are specific to the trap geometry and particle type used in this research.
Moreover, the strong agreement between the theoretical predictions and the simulations' results validates the computational model as a reliable tool. This makes it an effective method to investigate the Paul trap.

Despite successful radial confinement, the solution used to achieve axial confinement was proven insufficient. The simulation data show that the particle almost never remained trapped for longer than 500 μs, except for values of V_{slow}=1100 V and V_{fast}=100 V. The design adopted for the endcap electrodes was chosen to avoid interference with the light beam used in the optical trap, which likely limited the strength of the axial field. In a similar work, where a Paul trap is combined with an optical trap, axial confinement was achieved by applying a DC voltage to the optic's lens holders, located a distance 1.6 mm away from the trapcenter. The endcaps were supplied with a voltage of 70 V [13].
A possible solution to achieve axial confinement could be implementing parametric feedback cooling to the endcap electrodes. As described in the 'Theoretical Background' section, modulating the endcaps' potential in response to the particle's position could stabilize its motion along the z-axis.
In addition, implementing parametric feedback cooling to all the electrodes could enhance overall control over the particle, keeping its oscillation within a few micrometers from the trap center. This would facilitate re-trapping with the optical tweezer in the event of a drop.

Furthermore, in this study the maximum kinetic energy of the trapped nanoparticle was measured as a function of the *slow voltage* and for three different *fast voltage*. From the simulation data, it is found that the highest trap potential depth is achieved for a slow voltage of 1600 V and a fast voltage of 100 V. However, as previously stated, stable confinement along the three directions was not achieved for this configuration. For the case where 3D stable trapping was achieved, the nanoparticle's maximum kinetic energy is 256.0 eV. This suggests that the trap potential depth is at least higher than this value, otherwise the particle would have escaped the trapping region. This is in accordance with other works where the Paul trap's potential depth is measured to be around 1 keV [9].

A critical aspect encountered while doing the simulation was the computational time. Using the setting as described in the 'COMSOL Configuration for Simulations' section, each simulation took over six hours to compute, despite the FEM analysis was conducted using the coarsest mesh possible. This resulted in a delay in the data collection process, which ultimately reduced the available data. In future works, this problem can be overcome by adequately refining the mesh. The area of interest (i.e. the trapping region) should have a much finer mesh, while the surrounding space should have a coarser mesh, since this area is not of interest for the research. This adjustment could reduce the computational time while at the same time provide more accurate results.

The next phase of this research will explore the dual-frequency nature of the Paul trap to support experiments with multiple trapped particles. Such a configuration opens the door to investigating charged particle interactions. It also enables sympathetic cooling, where one particle species dissipates energy from another species, resulting in lower temperatures for both [16]. Furthermore, trapping ions together under this scheme can serve as a foundation for qubit implementation. In an another work, mixed-species ions where trapped simultaneously, where one species acts as a memory qubit and another as a communication qubit [17].

6 Conclusion

In this study, a dual-frequency RF Paul trap has been analyzed through computational simulations. The aim of the research was to find the optimal voltages and frequency to apply to the trap's electrodes, such that a charged nanoparticle of few hundreds of nanometer size could be trapped. This system is intended to serve both as a standalone trap and as a supplementary mechanism to optical tweezers, especially for recapturing particles that escape from optical confinement. Through a combination of theoretical analysis and finite element simulations in *COMSOL Multiphysics*, the optimal values of the voltage amplitudes and frequencies have been determined.

Stable confinement in the radial (xy) plane is achieved for an applied *fast voltage* of 100 V at a frequency of 20 MHz and values of the *slow voltage* in the range of 1000 V to 1600 V, oscillating at a frequency of 3 kHz. These conditions produced stability parameters within the bounded region predicted by the Mathieu stability diagram, demonstrating strong agreement between theory and simulation.
For axial (z-direction) confinement, a DC voltage of 50 V was applied to a pair of endcap electrodes. However, this solution only worked successfully for a *slow voltage* of 1100 V, and for a time interval of 700 μs. This highlights a limitation of the current electrode geometry and suggests that enhanced electrode design or active control methods are necessary to achieve reliable three-dimensional trapping over longer timescales.

The simulations also allowed for the estimation of the potential depth of the trap by analyzing the maximum kinetic energy of the confined nanoparticle. The deepest trap configuration corresponded to a slow voltage of 1600 V and a fast voltage of 100 V, with a maximum kinetic energy exceeding 550 eV. This aligns with reported values from experimental literature, where Paul traps are known to offer deep potential wells on the order of 1 keV.

In future experiments, the trap can be improved by implementing parametric feedback cooling to stabilize the particle motion along the three directions. Due to its dual-frequency nature, the Paul trap investigated could also be used for experiments that involve trapping different species of particles, such as an ion and a nanoparticle. These experiments can have multiple applications, especially in quantum computing technologies, sympathetic cooling and fundamental particle interactions.

Acknowledgments

I would like to express my gratitude to my supervisor, Steven Hoekstra, for the opportunity to work as part of his research team. His guidance, feedback, and support throughout the course of this project have been invaluable to my academic development. I am particularly grateful for the research project he assigned to me, which closely aligned with my interests in computational physics and allowed me to gain hands-on experience with advanced simulation and analysis tools. I would also like to extend my thanks to my daily supervisor, Bart Schellenberg, for his patience and consistent support. His willingness to answer all my questions and to walk me through complex ideas with clarity and detail has been essential to the progress of this work.
A special thank you goes to my parents, whose support and sacrifices have made it possible for me to pursue an undergraduate degree abroad.
Lastly, I acknowledge the use of Large Language Models (LLMs), such as ChatGPT, which were employed exclusively for language refinement, namely to help improve the clarity, coherence and grammar of the written text. All scientific content, data analysis, and interpretation are entirely my own.

Appendix

A Particle's Motion Graphs

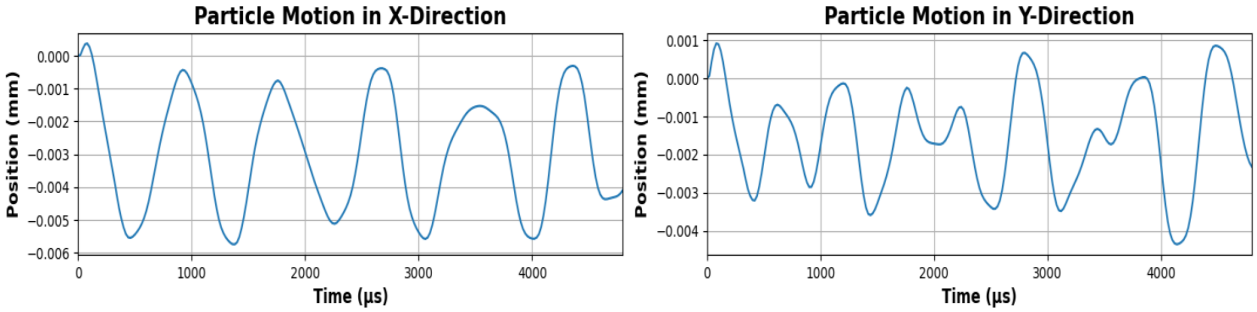

Figure 11: Graph of the particle's motion in the x- and y-direction for V_{slow}=1600 V. The trapping area's limits are $\pm$2.34 mm in the x-direction and $\pm$1.29 mm in the y-direction. Since the particle never goes beyond these limits, it is trapped. For values of V_{slow} smaller than 1600 V, the particle shows similar dynamics.

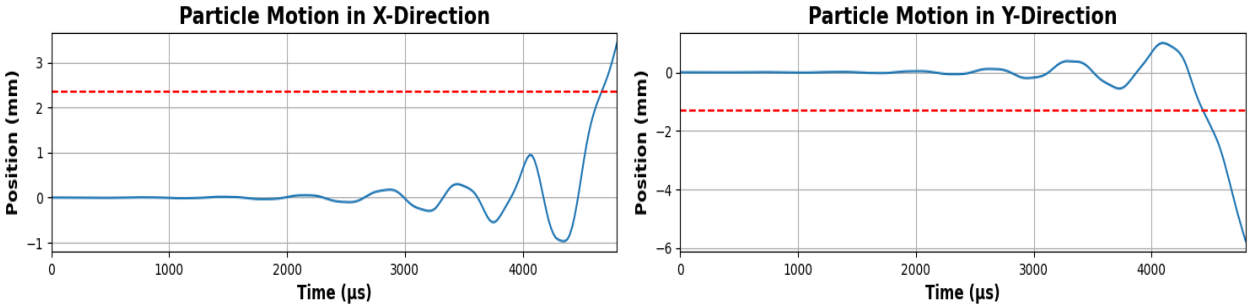

Figure 12: Graph of the particle's motion in the x- and y-direction for V_{slow}=1700 V. The trapping area's limits are represented by the dashed lines. Since the particle goes beyond these limits, it is not trapped. For values of V_{slow} bigger than 1700 V, the particle shows similar dynamics.

Figures of the particle's z-motion over a time range interval of 700 μs obtained from 3D simulations.

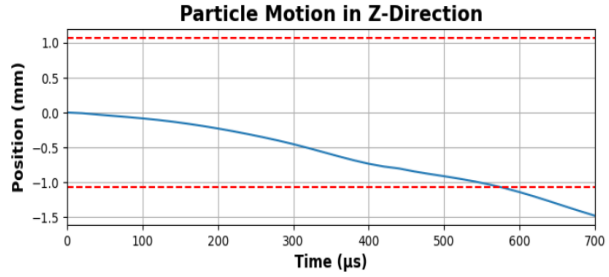

(a) Particle's motion for V_{slow}=1000 V.

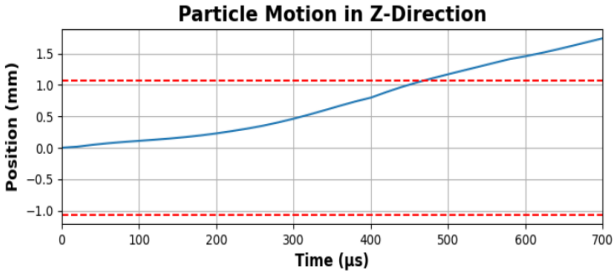

(b) Particle's motion for V_{slow}=1200 V.

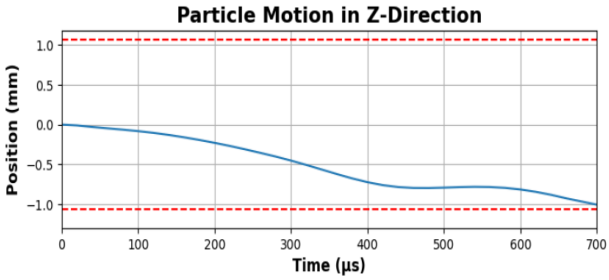

(c) Particle's motion for V_{slow}=1300 V.

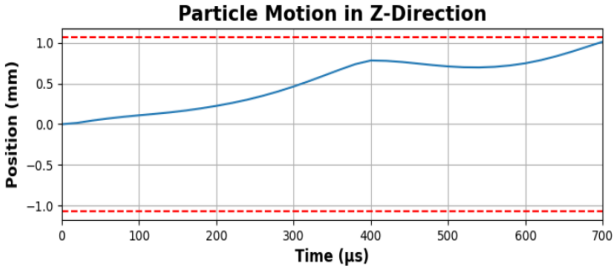

(d) Particle's motion for V_{slow}=1400 V.

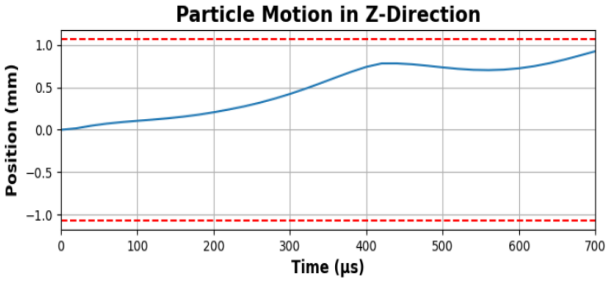

(e) Particle's motion for V_{slow}=1500 V.

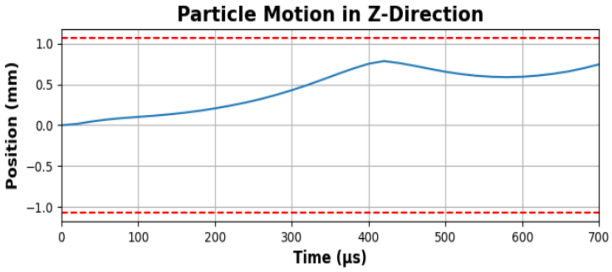

(f) Particle's motion for V_{slow}=1600 V.

Figure 13: Particle motion in z-direction for various V_{slow} values.

Bibliography

[1] M. Morshed Behbahani, *Dynamics of optically levitated nanoparticles*. PhD thesis, University of Groningen, (2024).

[2] R. Pushpa, R. D'Souza, and S. Ahmad, "Quadrupole ion traps," *Resonance*, vol. 6, pp. 22–37, (2001).

[3] J. Bruce, X. Cheng, R. Bakhtiar, Q. Wu, S. Hofstadler, G. Anderson, and R. Smith, "Trapping, detection, and mass measurement of individual ions in a fourier transform ion cyclotron resonance mass spectrometer," *Journal of the American Chemical Society*, vol. 116, no. 17, pp. 7839–7847, (1994).

[4] W.-P. Peng, Y.-C. Yang, M.-W. Kang, Y. T. Lee, and H.-C. Chang, "Measuring masses of single bacterial whole cells with a quadrupole ion trap," *Journal of the American Chemical Society*, vol. 126, no. 38, pp. 11766–11767, (2004).

[5] S. D. Fuerstenau, W. H. Benner, J. J. Thomas, C. Brugidou, B. Bothner, and G. Siuzdak, "Mass spectrometry of an intact virus," *Angewandte Chemie*, vol. 113, no. 3, pp. 559–562, (2001).

[6] J. N. Louris, J. W. Amy, T. Y. Ridley, and R. G. Cooks, "Injection of ions into a quadrupole ion trap mass spectrometer," *International Journal of Mass Spectrometry and Ion Processes*, vol. 88, pp. 97–111, (1989).

[7] P. Schindler, D. Nigg, T. Monz, J. T. Barreiro, E. Martinez, S. X. Wang, S. Quint, M. F. Brandl, V. Nebendahl, M. Roos, Christian F, M. Chwalla, R. Hennrich, and Blatt, "A quantum information processor with trapped ions," *New Journal of Physics*, vol. 15, no. 12, p. 123012, (2013).

[8] L. Magrini, P. Rosenzweig, C. Bach, A. Deutschmann-Olek, S. G. Hofer, S. Hong, N. Kiesel, A. Kugi, and M. Aspelmeyer, "Real-time optimal quantum control of mechanical motion at room temperature," *Nature*, vol. 595, no. 7867, pp. 373–377, (2021).

[9] D. S. Bykov, P. Mestres, L. Dania, L. Schmöger, and T. E. Northup, "Direct loading of nanoparticles under high vacuum into a paul trap for levitodynamical experiments," *Applied Physics Letters*, vol. 115, no. 3, (2019).

[10] J. Gieseler, B. Deutsch, R. Quidant, and L. Novotny, "Subkelvin parametric feedback cooling of a laser-trapped nanoparticle," *Physical review letters*, vol. 109, no. 10, p. 103603, (2012).

[11] D. S. Bykov, L. Dania, F. Goschin, and T. E. Northup, "A nanoparticle stored with an atomic ion in a linear paul trap," *arXiv preprint arXiv:2403.02034*, (2024).

[12] D. Trypogeorgos and C. J. Foot, "Co-trapping different species in ion traps using multiple radio frequencies," *Physical Review A*, vol. 94, no. 2, p. 023609, (2016).

[13] E. Bonvin, L. Devaud, M. Rossi, A. Militaru, L. Dania, D. S. Bykov, M. Teller, T. E. Northup, L. Novotny, and M. Frimmer, "Hybrid paul-optical trap with large optical access for levitated optomechanics," *Physical Review Research*, vol. 6, no. 4, p. 043129, (2024).

[14] D. J. Griffiths, *Introduction to electrodynamics*. Cambridge University Press, (2023).

[15] B. M. Mihalcea, "Mathieu–hill equation stability analysis for trapped ions: Anharmonic corrections for nonlinear electrodynamic traps," in *Photonics*, vol. 11, p. 551, (2024).

[16] D. Offenberg, C. Wellers, C. Zhang, B. Roth, and S. Schiller, "Measurement of small photodestruction rates of cold, charged biomolecules in an ion trap," *Journal of Physics B: Atomic, Molecular and Optical Physics*, vol. 42, no. 3, p. 035101, (2009).

[17] K. Sosnova, A. Carter, and C. Monroe, "Character of motional modes for entanglement and sympathetic cooling of mixed-species trapped-ion chains," *Physical Review A*, vol. 103, no. 1, p. 012610, (2021).